Unadulterated spectral function of low-energy quasiparticles in Bi$_2$Sr$_2$CaCu$_2$O$_{8+\delta}$

D. V. Evtushinsky,[1] A. A. Kordyuk,[1,2] S. V. Borisenko,[2] V. B. Zabolotnyy,[2] M. Knupfer,[2] J. Fink,[2] B. Büchner,[2] A. V. Pan,[3] A. Erb,[4] C. T. Lin,[5] and H. Berger[6]

[1]*Institute of Metal Physics of National Academy of Sciences of Ukraine, 03142 Kyiv, Ukraine*
[2]*IFW Dresden, P.O. Box 270116, D-01171 Dresden, Germany*
[3]*ISEM, University of Wollongong, Wollongong, NSW 2522, Australia*
[4]*Walther-Meißner-Institut, Bayerische Akademie der Wissenschaften, 85748 Garching, Germany*
[5]*Max-Planck Institut für Festkörperforschung, 70569 Stuttgart, Germany*
[6]*Institut de Physique de la Matiére Complexe, EPFL, 1015 Lausanne, Switzerland*

Fitting the momentum distribution photoemission spectra to the Voigt profile appears to be a robust procedure to purify the interaction effects from the experimental resolution. In application to Bi$_2$Sr$_2$CaCu$_2$O$_{8+\delta}$ high-T_c cuprates, the procedure reveals the *true* scattering rate at low binding energies and temperatures, and consequently, the true value of the elastic scattering. Reaching the minimal value $\sim$16 meV, the elastic scattering does not reveal a systematic dependence on doping level, but is rather sensitive to impurity concentration and can be explained by the forward scattering on out-of-plane impurities. The inelastic scattering is found to form well-defined quasiparticles with the scattering rate $\sim\omega^2$ and $\sim\omega^3$, above and below T_c, respectively.

A century ago, in the time of the renowned Kamerlingh Onnes's experiments, the search for actual behavior of electrical conductivity in pure metals at low temperature led to the discovery of superconductivity.[1] Today, a similar problem, the low temperature/energy behavior of normal electrical conductivity is topical again, now for high-T_c cuprates (HTSC). The quantity of special interest is a quasiparticle scattering rate $1/\tau$,[2] or, more precisely, the single-particle self-energy, $\Sigma = \Sigma' + i\Sigma''$,[3] the real part of which can be associated with the mass renormalization and the imaginary part is proportional to the scattering rate or, in the simplest Drude model, to the normal-state resistivity. The true lowest value of Σ'' (taken at the Fermi level) is important to know in order to reconcile the parameters of quasiparticle spectrum with transport measurements, but its asymptotic behavior, i.e., $\Sigma''(\omega, T)$ at low energy and temperature, is vital to judge whether the quasiparticle approach is applicable at all to describe the electronic properties of HTSC.

The self-energy function $\Sigma(\omega, T)$ is closely related to (and can be derived from) the quasiparticle spectrum, presented by the quasiparticle spectral function $A(\mathbf{k}, \omega, T)$, which, in turn can be mapped accurately in the whole Brillouin zone (BZ) by modern angle-resolved photoemission spectroscopy (ARPES).[4] For the nodal direction, along which the superconducting d-wave gap function has a node (i.e., changes sign), all the interactions which form the nodal quasiparticles are encapsulated in Σ, both parts of which can be confidently determined from ARPES spectra in the range about 0.3 eV below the Fermi level.[5,6] Nevertheless, the detailed behavior of $A(\omega, T)$ and $\Sigma(\omega, T)$ in the very vicinity to E_F remains puzzling. The experimental resolution, which can be safely neglected for higher binding energy, plays a crucial role here. Roughly, the photocurrent intensity can be well approximated by a convolution of the spectral function, multiplied by the Fermi-function $f(\omega)$, and overall experimental resolution:[7]

$$I(\mathbf{k}, \omega) \propto A(\mathbf{k}, \omega) f(\omega) \otimes R(\mathbf{k}, \omega). \quad (1)$$

The latter consists of two essential components, the response function of the analyzer, $R_A(\mathbf{k}, \omega)$, and one which accounts for inhomogeneities of sample surface $R_S(\mathbf{k}, \omega)$: $R = R_A \otimes R_S$. While the analyzer response function is fixed and can be measured independently, the surface inhomogeneities (mechanical, chemical, or in charge distribution) result in a systematic error, which is difficult to account for. This seemingly technical problem has a rather strong fundamental impact, setting an unavoidable limit for Σ'' estimation accuracy. In this paper we show that using a simple line-shape analysis—namely, a Voigt fitting procedure—one can purify the intrinsic interaction effects from the extrinsic influence of the experimental setup and, therefore, uncover true parameters of the low-energy part of a quasiparticle spectrum. Applying the procedure to the nodal photoemission spectra from Bi$_2$Sr$_2$CaCu$_2$O$_{8+\delta}$ (Bi-2212), we determine true values of the impurity scattering, as well as the energy and temperature dependence of the scattering rate in close vicinity to the Fermi level.

We analyze the spectra from pure Bi-2212, lead-doped superstructure-free Bi(Pb)-2212,[5–9] as well as Bi-2212 doped with Zn and Ni.[10] Here we focus on the spectra measured along the nodal (π, π) direction where the 5×1 superstructure is well resolved[11] and at 27 eV excitation energy at which the contribution from the bonding band is essentially suppressed.[9] The experimental details can be found elsewhere.[5,7–10]

Figure 1(a) introduces the essentials of the nodal spectra analysis. The blurred region represents the "ARPES image"—the photocurrent intensity $I(k, \omega)$, which over the occupied states can be well approximated by the quasiparticle spectral function
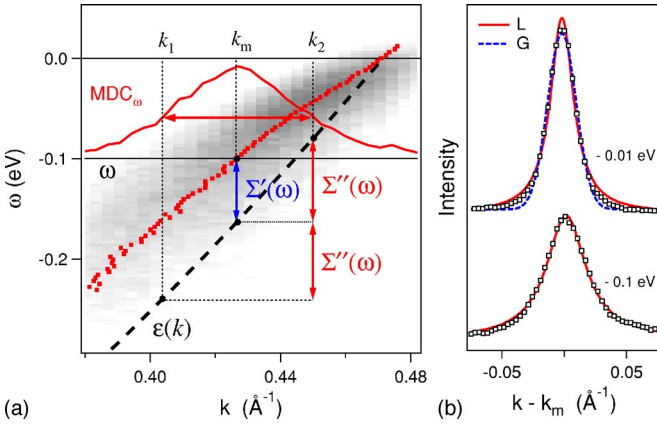
FIG. 1. (Color online) (a) Nodal spectra parameters: Bare-band dispersion (dashed line) and renormalized dispersion (points) on top of the spectral weight of interacting electrons ("ARPES image"). The solid line represents a single MDC at ω, arrows indicate its FWHM, and the self-energy parts derived for a given MDC. (b) Two MDC's taken at -0.1 and -0.01 eV, and their fits to Lorentzian (solid lines) and Gaussian (dashed line) functions.

$$A(k,\omega) = -\frac{1}{\pi}\frac{\Sigma''(\omega)}{[\omega - \varepsilon(k) - \Sigma'(\omega)]^2 + \Sigma''(\omega)^2}, \qquad (2)$$

where $\varepsilon(k)$ is the bare band dispersion along the nodal direction. Since the ARPES image became a unit of information in modern photoemission, the advantages of the analysis of the ARPES spectra in terms of the momentum distribution curves (MDC), MDC$\equiv I(k,\omega{=}\mathrm{const})$, had been immediately realized.[12] The main advantage comes from the fact that $A(k)$ has a simple Lorentzian line shape as long as momentum dependence of the self-energy and bare Fermi velocity, $v_F = d\varepsilon(k)/dk$, can be neglected.[13] The latter, as well as Eq. (1), has been shown to be valid for the nodal direction of Bi-2212 up to 0.3 eV binding energy by means of Kramers-Kronig self-consistency of the self-energy parts.[5] The relations of bare dispersion and self-energy parts with the parameters of an MDC at given ω are shown in Fig. 1(a), though, in this paper we focus in Σ'', which at low binding energy is simply proportional to the MDC width (half width at half maximum): $\Sigma'' = v_F W$.

The analysis presented in Ref. 5 also allows us to estimate the contribution of the experimental resolution, although due to a number of parameters involved, such an estimate is not very precise. Fortunately, the close similarity between $I(k,\omega)$ and $A(k,\omega)$ at higher binding energies suggests the way to recover true quasiparticle spectrum also in close vicinity to E_F. It was noticed[14] that, when approaching the Fermi level, the line shape of MDC measured along the nodal direction evolves from almost ideal Lorentzian to more Gaussian-type, which evidently, is a result of the convolution of the photo-emission signal with the total response function of the setup. Figure 1 illustrates such a Lorentzian to Gaussian crossover: While the MDC taken at $\omega{=}{-}0.1$ eV is almost perfect Lorentzian, the MDC measured closer to the Fermi level at $\omega{=}{-}0.01$ eV can be fitted to neither Lorentzian nor Gaussian but to a convolution of these two—the Voigt profile.
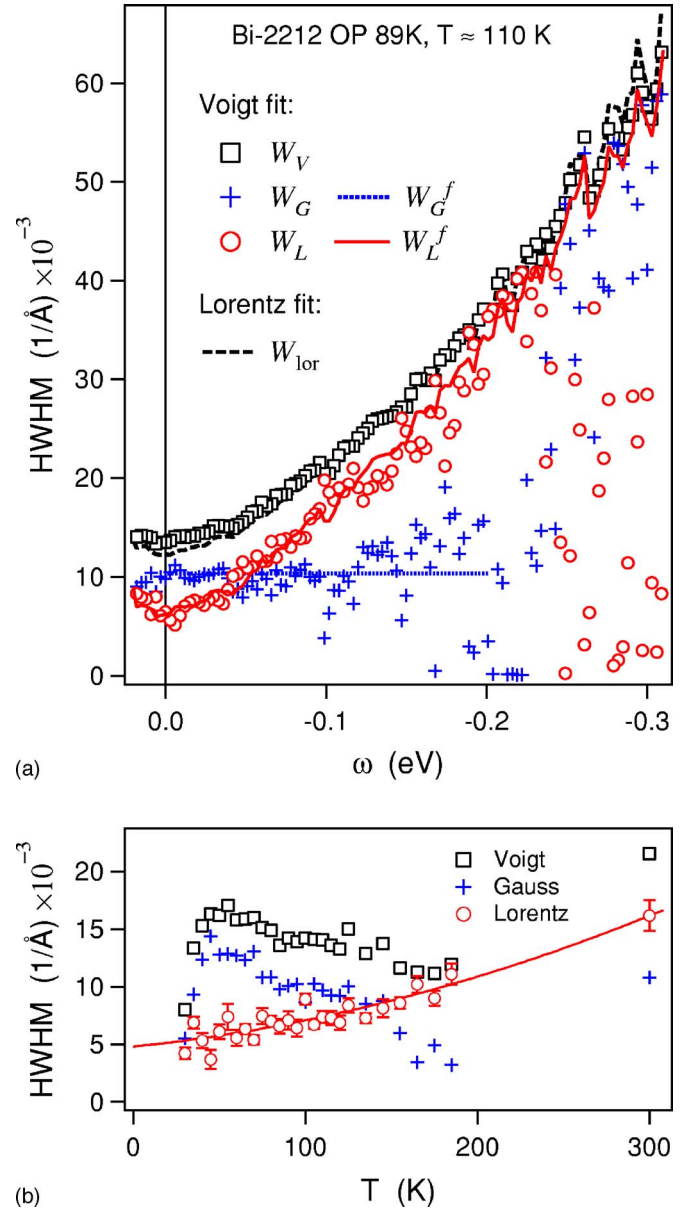

FIG. 2. (Color online) Constituents of MDC width: (a) energy dependence of MDC width presented by half width at half maximum (HWHM) of its fit to the Voight profile W_V (W_{Lor} is the result of simple Lorentzian fit), and its Lorentzian W_L, and Gaussian W_G constituents; (b) variation of the above-mentioned parameters (at $\omega{=}0$) with temperature.

Figure 2 illustrates effectiveness of the fitting procedure for the nodal spectra analysis. The parameters of the fit are shown in Fig. 2(a) as a function of energy for the Bi-2212 OP89 sample measured above T_c. Here W_V is the width of the Voigt profile, while W_L and W_G are the widths of its constituents, the Lorentzian and Gaussian, respectively. W_{Lor} represents the "traditional" MDC width used in previous data analysis—the width of the Lorentzian from the pure Lorentzian fit. Fitting MDC's to the Voigt profile instead of to the Lorentzian introduces one additional parameter, W_G. In the fitting procedure we use the Voigt function[15] implemented in IGOR Pro (Wavemetrics Inc.), which can be approximated
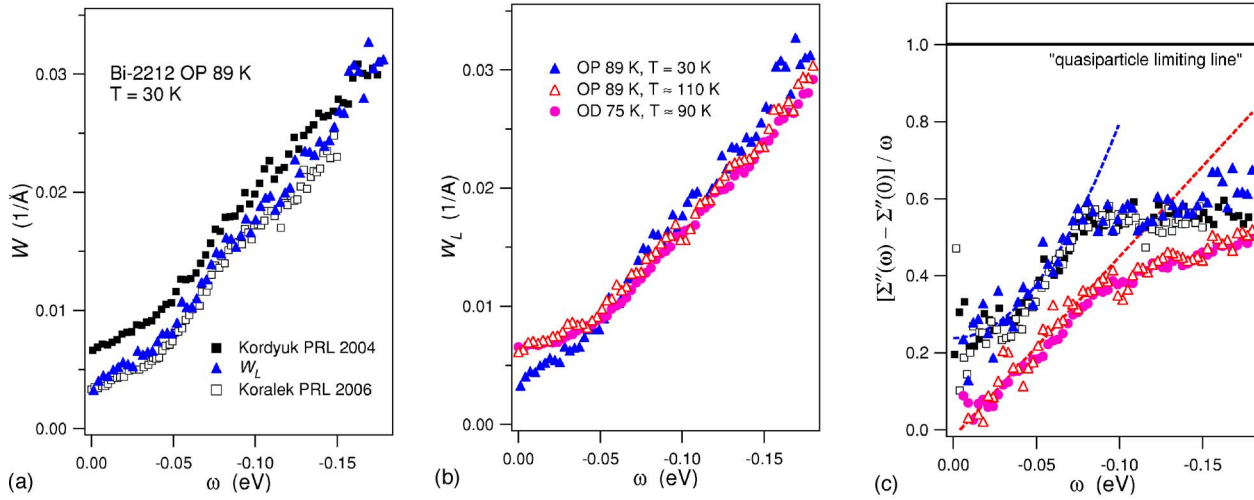
FIG. 3. (Color online) Energy dependence of the scattering rate. (a) Optimally doped Bi-2212 below T_c: MDC width (HWHM) measured with 27 eV synchrotron radiation (Ref. 8) (filled squares) and the true width of the quasiparticle spectrum for the same sample purified from the resolution effect (filled triangles), to compare to the data for a similar sample measured with 6 eV laser light (Ref. 16) (open squares). (b) Evolution of $W(\omega)$ with increasing temperature and overdoping. (c) The same data shown in a reduced dimensionless scale, dashed lines represent a parabolic fit to the low-T data and a linear fit to the high-T data, respectively.

by a simple relation between the above-mentioned parameters;

$$W_V = V(W_L, W_G) = \frac{W_L}{2} + \sqrt{\frac{W_L^2}{4} + W_G^2}. \quad (3)$$

Deviation of this approximation from real convolution is maximal when $W_L \approx W_G$ but is less than 1.2%.

As it is expected for contribution of the experimental resolution, the Gaussian width is essentially ω independent in the actual range of interest, $-0.1\ \text{eV} < \omega < 0\ \text{eV}$: $W_G(\omega) = W_G^f$. So, the energy dependence of W_V is accumulated in W_L, which represents now a *true* width of the quasiparticle spectral function. At energies $\omega < -0.15$ eV, due to critical lowering of the signal-to-noise ratio, the fit becomes unstable in distinguishing the line-shape type. Therefore, in order to reduce the experimental uncertainty we fit the $W_G(\omega)$ to W_G^f on $[-0.1, 0]$ eV energy range and define the true Lorentzian widths W_L^f from Eq. (3): $W_V = V(W_L^f, W_G^f)$. In the following, we omit "f" but discuss exactly the $W_L^f(\omega)$ function as the most careful representative of the true scattering rate.

Figure 2(b) represents not a usual but an interesting example that demonstrates the efficiency of the Voigt fitting procedure. It shows the values $W_V(0)$, $W_L(0)$, and W_G determined for the same sample at different temperatures. In this case, the APRES spectra have been measured during heating that implies a motion of the sample in respect to the beam spot due to thermal expansion of the manipulator. Evidently, this has resulted in different angular resolution in each point, which appeared as a random distribution of $W_G(T)$ while the recovered $W_L(T)$ function has been found to be monotonic.

We have applied the procedure to a number of ARPES spectra taken from Bi-2212 samples of different doping levels at different temperatures. In the following, we discuss the energy dependence of the true scattering rate $W_L(\omega)$, its zero energy value $W_L(0)$, and its dependence on doping and temperature.

In respect to the $W_L(\omega)$ problem, Eq. (3) helps to make an important remark. In a low scattering limit, when $W_L \ll W_G$, $W_V \approx W_G + W_L/2$. In other words, if for example, $W_L(\omega) \propto \omega$, such a linear dependence cannot be camouflaged by the resolution.

With Fig. 3 we discuss the *energy dependence* of the scattering rate. In panel (a) we compare the MDC width for the OP89 sample, measured below T_c with 27 eV synchrotron radiation,[8] to the data for the near-optimally doped Bi-2212, measured with 6 eV laser light.[16] Besides different offsets, two data sets look very similar [see also panel (c)]. Moreover, when the width of the quasiparticle spectrum for the OP89 sample is purified from the resolution effect, it almost coincides with the laser data. This supports the conclusions about validity of the sudden approximation. Slightly higher scattering (taking into account a finite resolution in laser data) can be explained by an influence of the elastic surface scattering on quasiparticles in the topmost CuO bilayer.

To reveal the asymptotic behavior of the scattering rate at low energy, in panel (c) we replot these data in the form of $\sigma''(\omega) = [\Sigma''(\omega) - \Sigma''(0)]/\omega$. To get Σ'' we just multiply W_L by $v_F = 4$ eV Å.[5] One can see that below T_c at low energy, $\sigma''(\omega)$ has a nonvanishing offset and a quadratic term. In $\Sigma''(\omega)$, these terms correspond to $\sim \omega$ and $\sim \omega^3$ terms, respectively, recently also observed elsewhere.[17] At higher temperatures and hole doping [see panels (b) and (c)], $\Sigma''(\omega)$ becomes purely quadratic. Both terms are a simple consequence of the modified density of states (DOS) below T_c: d-wave superconducting gap makes the DOS linear at low $|\omega|$. The ω term is expected for the elastic scattering.[19] Examining two extremes, the forward and backward (isotropic) scattering, we note that it is the former which should not noticeably effect
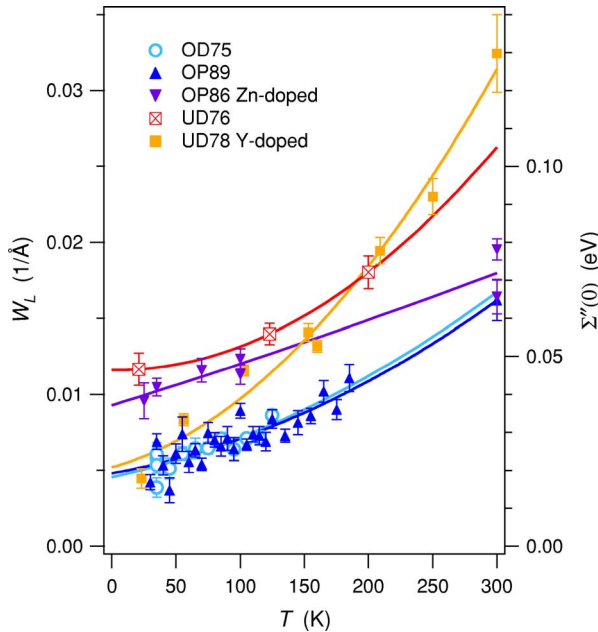
FIG. 4. (Color online) Temperature dependence of the scattering rate at $\omega=0$. Error bars are determined by mean-square deviation of W_G^f; solid lines show the second-order polynomial fit.

the d-wave superconductivity (linear DOS), as the later does. Therefore, we can conclude that the main contribution to Σ'' at low T and $|\omega|$ comes from the forward impurity scattering while the influence of the isotropic scattering is negligible. The same mechanism is responsible for the evolution of the ω^2 inelastic scattering above T_c (Refs. 6 and 8) into the ω^3 term below T_c. Thus, in both the normal and superconducting state the inelastic scattering is the one that forms well-defined quasiparticles also at optimal doping. In panel (c), we also draw the "quasiparticle limiting line" to show how, in fact, well defined are the nodal quasiparticles in the optimally doped Bi-2212.

Now we discuss the *residual scattering* at $\omega \rightarrow 0$ and $T \rightarrow 0$: $\Sigma_0'' = v_F W_L(0,0)$. Figure 4 shows $W_L(0,T)$ dependences for several samples. The resolution-purified residual (Σ_0''

> 16 meV or $W_L(0,0) > 4 \times 10^{-3}$ Å^{-1}) is more than seven times lower now than the values that have been used earlier[20] to compare ARPES and transport measurements, but is still much higher than a reasonable estimate $(1-2$ meV) for the isotropic unitary scattering.[19,21] Therefore, although we can conclude that Σ_0'' does not show a systematic dependence on doping level (OD75, OP89, and UD78 samples in Fig. 4) but is just sensitive to impurity concentration (here UD76 represents a sample, highly underdoped by annealing in He, which removes out-of-plane oxygen, while the OP86 the sample doped with 1% of Zn gives an example of the in-plane impurity), the comparison to transport (the contribution of the forward scattering to which is negligible) is still problematic. In order to do such a comparison, the way to determine the isotropic constituent of the impurity scattering in ARPES should be elaborated.

The *temperature dependence* of Σ'' deserves a separate investigation. One of the surprising results is that, within the accuracy ~ 10 meV, there is no drop of Σ'' at T_c, such as reported recently in Refs. 17 and 18. The absence of the pronounced drop can be a consequence of the pseudogap, which smoothes the T dependence of the phase space available for scattering. The essential (~ 20 meV) drop, observed in Ref. 17, might be because the analyzed spectrum was not measured along the nodal direction. It is also important to understand the reason for the different dependences presented in Fig. 4. While for most samples the variation in $\Sigma''(0,T)$ can be explained by different scattering on impurities, the much stronger T dependence for the Y-doped sample needs further study.

The questions which we left open, an accurate (x,T) dependence of the residual scattering rate and the evaluation of the isotropic impurity scattering, evidently require data of much better accuracy. In this respect, the described procedure transfers the uncontrolled systematic sample-related error into the random one, which can be made infinitesimal simply by increasing the time of spectra recording.

[1] W. Buckel, *Superconductivity: Fundamentals and Applications* (VCH, Weinheim, 1991).

[2] Here we call "quasiparticles" any elementary electronic excitations that can be described in terms of Dyson self-energy. The excitations with a nonzero coherent component[3] we will call "well-defined quasiparticles."

[3] S. Hüfner, in *Photoelectron Spectroscopy*, Springer Series in Solid State Sciences, Vol. 82 (Springer-Verlag, Berlin, 1995).

[4] For a review see A. Damascelli, Z. Hussain, and Z.-X. Shen, Rev. Mod. Phys. **75**, 473 (2003).

[5] A. A. Kordyuk et al., Phys. Rev. B **71**, 214513 (2005).

[6] A. A. Kordyuk et al., Phys. Rev. Lett. **97**, 017002 (2006).

[7] S. V. Borisenko et al., Phys. Rev. B **64**, 094513 (2001).

[8] A. A. Kordyuk et al., Phys. Rev. Lett. **92**, 257006 (2004).

[9] A. A. Kordyuk et al., Phys. Rev. B **70**, 214525 (2004).

[10] V. B. Zabolotnyy et al., Phys. Rev. Lett. **96**, 037003 (2006).

[11] S. V. Borisenko et al., Phys. Rev. Lett. **84**, 4453 (2000).

[12] T. Valla et al., Science **285**, 2110 (1999).

[13] More generally, one has to neglect $d^2\Sigma'(k)/dk^2$ and $d\Sigma''(k)/dk$ [see M. Randeria, A. Paramekanti, and N. Trivedi, Phys. Rev. B **69**, 144509 (2004)].

[14] A. A. Kordyuk and S. V. Borisenko, cond-mat/0510421 (unpublished).

[15] F. Schreier, J. Quant. Spectrosc. Radiat. Transf. **48**, 743 (1992).

[16] J. D. Koralek et al., Phys. Rev. Lett. **96**, 017005 (2006).

[17] T. Valla et al., Phys. Rev. B **73**, 184518 (2006).

[18] T. Yamasaki et al., cond-mat/0603006 (unpublished).

[19] T. Dahm, P. J. Hirschfeld, D. J. Scalapino, and L. Zhu, Phys. Rev. B **72**, 214512 (2005).

[20] T. Yoshida et al., Physica B **351**, 250 (2004).

[21] P. J. Hirschfeld, W. O. Putikka, and D. J. Scalapino, Phys. Rev. B **50**, 10250 (1994).